ISSN 0016-7029, Geochemistry International, 2006, Vol. 44, No. 12, pp. 1157–1169. © Pleiades Publishing, Inc., 2006.
Original Russian Text © V.P. Simanenko, V.V. Golozubov, V.G. Sakhno, 2006, published in Geokhimiya, 2006, No. 12, pp. 1251–1265.

Geochemistry of Volcanic Rocks from Transform Margins: Evidence from the Alchan Basin, Northwestern Primorie

V. P. Simanenko, V. V. Golozubov, and V. G. Sakhno

Far East Geological Institute, Far East Division, Russian Academy of Sciences, pr. Stoletiya Vladivostoka 159, Vladivostok, 690022 Russia

e-mail: sim-vp@mail.ru

Received February 15, 2005

Abstract—Geological, petrochemical, and geochemical data are reported for volcanic rocks of a Cretaceous pull-apart basin in the Tan Lu strike-slip system, Asian continental margin. A comparison of these volcanic rocks with magmatic rocks from typical Cenozoic transform margins in western North America and rift zones of Korea made it possible to distinguish some indicator features of transform-margin volcanic rocks. Magmatic rocks from strike-slip extension zones bear island-arc, within-plate, and, occasionally, depleted MORB geochemical signatures. In addition to calc-alkaline rocks, there are bimodal volcanic series. The rocks are characterized by high K_2O, MgO, and TiO_2 contents. They show variable enrichment in LILE relative to HFSE, which is typical of island-arc magmas. At the same time, they are rich in compatible transition elements, which is a characteristic of within-plate magmas. The trace-element distribution patterns normalized to MORB or primitive mantle usually display a negative Ta–Nb anomaly typical of suprasubduction settings. Their Ta/Nb ratio is lower, whereas Ba/Nb, Ba/La, and La/Yb are higher than those of some MORB and OIB. In terms of trace-element systematics, for example, Ta–Th–Hf, Ba/La–$(Ba/La)_n$, $(La/Sm)_n$–La/Hf, and others, they fall within the area of mixing of magmas from several sources (island arc, within plate, and depleted reservoirs). The magmatic rocks of transform settings display a sigmoidal chondrite-normalized REE distribution pattern, with a negative slope of LREE, depletion in MREE, and an enriched or flat HREE pattern. The magmas with mixed geochemical characteristics presumably originated in a transform margin setting in local extension zones under the influence of mantle diapirs, which caused metasomatism and melting of the lithosphere at different levels, and mixing of melts from different sources in variable proportions.

DOI: 10.1134/S0016702906120019

INTRODUCTION

From the Early Cretaceous to Paleogene, the eastern margin of Asia was probably a Californian-type transform continental margin [1]. Transform interaction between oceanic and continental plates caused large-scale strike-slip movements along the Asian margin and formation of numerous pull-apart basins in northeastern China, Korea, and Primorie [2–6]. The opening of these basins and filling with sediments were often associated with intense volcanism. The processes of opening and filling of the basins were described in detail, whereas data on magmatism are almost absent. Exceptions are the Paleogene depressions of Korea, which formed under strike-slip conditions in the Cenozoic transform margin of Asia. Their magmatism was recently described in several publications [7–9]. As to the Early Cretaceous depressions, preliminary data are available only for the Albian–Cenomanian volcanic rocks of the Partizanskii coal basin, southern Primorie [10].

This paper presents data on Cretaceous magmatism of the Alchan basin, northwestern Primorie, compared with magmatic rocks from typical transform settings of western North America, Cenozoic depressions of Korea, and Middle Cretaceous volcanic rocks of the Partizanskii basin. The goal of this study was to reveal the geochemical indicators of magmatism in a transform setting.

METHODS

Major elements were analyzed by conventional chemical techniques at the laboratories of the Far East Geological Institute, Far East Division, Russian Academy of Sciences (analysts V.U. Kramarenko and L.V. Nedashkovskaya). The concentrations of trace elements were determined by ICP-MS at the Laboratory of Isotopy and Geochronology, Institute of the Earth's Crust, Siberian Division, Russian Academy of Sciences (Irkutsk). The chemical preparation of samples for trace-element analysis was conducted using doubly distilled water from deep levels of Lake Baikal. Ultrapure acids purified twice by isothermal distillation were used for sample preparation. Hydrofluoric acid was purified in a Teflon apparatus, and H_2O, HNO_3, and HCl were purified in a quartz apparatus. ICP-MS analysis was conducted using a VG Plasmaquad PQ2+ mass

spectrometer at the Irkutsk Cooperative Analytical Center. The instrument was calibrated using the BHVO-1, AGV-1, and BIR-1 international standards, and sample U-94-5 (basanite) was used as an internal laboratory standard to monitor the quality of analysis.

GEOLOGY OF THE ALCHAN BASIN

The Alchan basin [11] was formed mainly in the Aptian–Cenomanian at the juncture of the Alchan and Arsen'ev faults belonging to the Tan Lu strike-slip system [3, 4, 6] (Fig. 1). The basin is located in the northeastern part of the Khanka Massif at its junction with the Samarka terrane. In plan view the basin is a triangle extending in the northeastern direction; its acute angle is located in the upper reaches of the Matai River, and the major portion lies in the Alchan River basin (right tributary of the Bikin River) and the watershed of the Bikin and Bol'shaya Ussurka. The basin is ~6300 km^2 in area. Its basement is made up of the Precambrian–Early Paleozoic rocks of the Khanka Massif, which are overlain in places by Late Permian, Triassic, and Jurassic terrigenous rocks.

The basin consists of the Zmeya–Stolbov and Guber volcanic grabens, which developed more or less independently, separated by the Silan'shan horst. The latter is separated by the Kedrach overthrust from the Guber graben and by the Silan'shan strike-slip fault with down-dip displacement from the Zmeya–Stolbov graben (Fig. 1).

Volcanic and volcanosedimentary sequences were accumulated in the Alchan basin mainly in the Albian–Cenomanian, i.e., during the most intense sinistral strike-slip motion along the entire Tan Lu fault system [12]. They are represented by the Assikaev and Alchan formations and Stolbov sequence [13].

From the Middle Cenomanian to the end of the Late Cretaceous, a change in the direction of motion of the Izanaga plate adjoining the Asian continent [14] caused the resumption of subduction processes. As a result, Andean-type continental margin environments are reconstructed in most parts of the eastern margin of Asia.

Active tectonic processes and dextral strike-slip movements along the Tan Lu fault system resumed at the end of the Late Cretaceous to the beginning of the Paleogene [12]. Extension related to strike-slip motion in various parts of the Asian continental margin was associated with local basaltic andesite and andesite volcanism. In particular, the andesites of the Severyanka Formation erupted in the Alchan basin. These volcanic rocks were previously considered as subduction-related and comparable with the Maastrichtian andesites of the Samarga Formation in the Eastern Sikhote Alin belt.

The Assikaev Formation occurs in the central part of the Alchan basin, in the framing of the Silan'shan horst (Fig. 1) and is subdivided into three subformations. The lower Assikaev subformation (780 m) consists of tuffaceous sandstones with lenses of carbonaceous mudstones and coals. The middle Assikaev subformation (870 m) is dominated by siltstones with sandstone intercalations. Flows of spilitic basalts were found among the deposits of this formation near the settlement of Verkhnii Pereval [15]. The upper Assikaev subformation (~850 m) is dominated by sandstones, which grade upward into a rhythmic intercalation of sandstones and siltstones. Ash-rich coal beds with intercalations of psammitic dacite tuffs occur in the upper part of the subformation in the eastern part of the basin. The formation was formed in a coastal marine setting during the late Aptian to middle Albian [13].

The Alchan Formation is mainly volcanogenic and fills the major portion of the Alchan basin. The volcanogenic complex includes vents, extrusive and subvolcanic bodies, lavas, tuffs, and ignimbrite flows of volcanic slopes, as well as tuffites, tuffstones, and siltstones of distal facies. The Alchan volcanic activity occurred in two cycles, which were separated by the sedimentation of terrigenous rocks. These cycles correspond to the lower and upper Alchan subformations.

The structure and composition of volcanic rocks of the formation vary significantly within the main tectonic units of the basin. In the Zmeya–Stolbov graben, the lower Alchan subformation conformably overlies the upper Assikaev subformation and is composed of ignimbrites, brecciated lavas, and tuffs of dacites and rhyodacites, up to 800 m thick. The upper Alchan subformation (up to 800 m) consists of intercalated volcanosedimentary rocks and dacite tuffs. A siltstone bed, up to 90 m thick, is ubiquitous at the roof of dacites [13]. In the Guber graben, the lower Alchan subformation rests unconformably on the rocks of the Pre-Cretaceous basement. Its lower part (135–450 m) is composed of tuffaceous sandstones and siltstones intercalated with dacite tuffs, and its upper part (600–900 m) is composed of a member of tuffs and brecciated dacite lavas. The upper Alchan subformation is 600–900 m thick and made up of alternating andesite lavas and tuffs, from 5–10 to 80–110 m thick. Thin dacite flows were observed in the upper part of the upper Alchan subformation. Within the Silan'shan horst, the lower Alchan subformation lies on the middle Assikaev subformation with erosion and azimuthal and angle unconformity [13]. The base of subformation is composed of a 14.5-m-thick layer of conglomerates, siltstones, and carbonaceous mudstones with plant fossils. The major portion of the subformation (370 m) is made up of dacitic ignimbrite flows. The upper Alchan subformation is composed there of andesite tuffs and lavas (160 m thick) changing upward by dacitic tuffs and ignimbrites intercalated with tuffites (720 m).

The Alchan Formation was formed in a continental setting; plant and faunal fossils indicate the second half of the middle Albian and the late Albian [13, 16–18].

The Stolbov sequence (900 m) occurs locally in two depressions in the Zmeya–Stolbov and Guber gra-

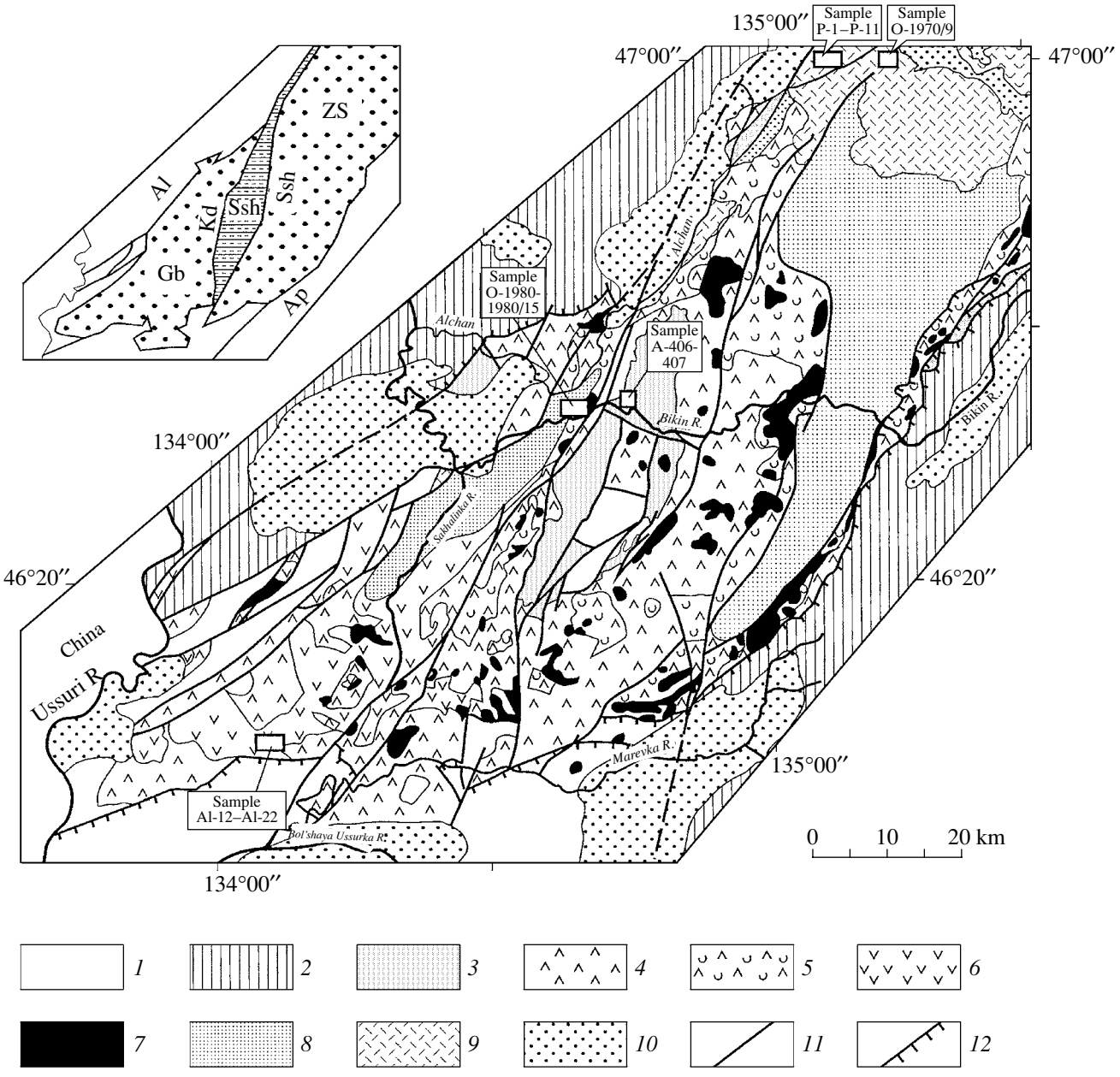

Fig. 1. Geological map of the central and southern parts of the Alchan basin (Golozubov et al., 2002) with sampling sites. (*1*, *2*) Complexes of the Pre-Cretaceous basement: (*1*) Precambrian metamorphic and igneous rocks of the Khanka superterrane overlain by the cover of mainly terrigenous Late Permian, Triassic, and Jurassic rocks; (*2*) Jurassic mixtites with slices of ophiolites, flints, and basalts of the Samarka terrane; (*3*) terrigenous rocks of the Assikaev Formation (Aptian–lower Albian); (*4–6*) volcanic rocks of the Alchan Formation (middle and upper Albian): (*4*) tuffs, ignimbrites, and lavas of dacites, rhyodacites, and more rare rhyolites, with tuffite intercalations (lower subformation), (*5*, *6*) volcanic rocks of the upper subformation: (*5*) dacite, rhyodacite tuffs and tuffites, (*6*) andesite tuffs and lavas; (*7*) Alchan volcanic rocks of the subvolcanic, extrusive, and vent facies; (*8*) terrigenous variegated rocks of the Stolbov sequence (Cenomanian); (*9*) Late Cretaceous (Maastrichtian) volcanic rocks of the Severyanka Formation; (*10*) Tertiary depressions; (*11*) sinistral strike-slip fault; (*12*) normal faults and overthrusts. The inset shows the location of main structures of the Alchan basin: (Gb) Guber graben, (Ssh) Silanshan horst, and (ZS) Zmeya–Stolbov graben; faults: (Al) Alchan, (Kd) Kedrach, (Ssh) Silanshan, and (Ar) Arsen'ev.

bens. In both depressions, the sequence has a similar structure and consists of alluvial and lacustrine deposits: conglomerates, gritstones, sandstones, variegated and red siltstones. These rocks were deposited under semi-arid conditions with a minor contribution from volcanic activity. Palinological data, plant fossils, and fresh-water Crustacea indicate its Cenomanian age [13, 16].

The Severyanka Formation. The volcanic rocks of the formation occur along right tributaries of the Bikin

River in the Alchan River basin, where they compose apronlike flows in the Alchan and Bikin troughs. The volcanic rocks of the Severyanka Formation are separated by an erosion surface from the Alchan Formation. The formation is composed mainly of lava flows of andesites, basaltic andesites, and basalts. Subordinate tuffs (<10 vol %) occur sporadically as layers of variable thickness between lava flows. No compositional trend was observed throughout the section which begins from andesites in the left bank of the Alchan River and from basaltic andesites and basalts (unpublished data of B.A. Kabanov et al., 1987) in Oktyabr'skaya Mt. The thickness of lava flows varies from 5–8 to 40–50 m. The volcanic rocks associate with numerous small intrusive bodies and stocks of andesite and dacite compositions. Floral and paleomagnetic data testify to the Maastrichtian age of the formation (unpublished data of B.A. Kabanov et al., 1987).

PETROGRAPHY AND GEOCHEMISTRY

The basalts of the Assikaev Formation are spilitized clinopyroxene–plagiophyric rocks. They show high alkali ($K_2O + Na_2O > 5$ wt %), moderate Al_2O_3, and low TiO_2 contents (0.75–0.85%) and pertain to the trachybasalt K–Na subalkaline series with $K_2O/Na_2O \sim 1$ (Table 1, Fig. 2).

The lower Alchan subformation shows initial silicic eruptions followed by more basic volcanic rocks. It is mainly composed of pyroclastic rocks (ignimbrites, tuffs and tuffolavas of dacites, rhyodacites, and rhyolites) with sharply subordinate lavas. The ignimbrites are characterized by a varying degree of welding and are grouped on the basis of the distribution of clasts (10–70%) into vitric, lithic, and other types. Their crystal clasts are plagioclase (from oligoclase to labradorite), quartz, biotite, hornblende, and pyroxene in variable proportions. The groundmass is a variably welded ash material, occasionally with a well-expressed pseudofluidal texture. The dacite and rhyolite tuffolavas have porphyroclastic and lithoclastic textures. Their crystal clasts are albitized and sericitized plagioclase and K-feldspar. In addition to quartz, the silicic rocks contain sanidine, biotite, hornblende, and pyroxene. The accessory minerals are zircon, apatite, and Ti-magnetite. The cement is represented by a partially devitrified fluidal glass. The same phenocrysts were observed in the fluidal glass of the dacite and rhyolite lavas, but they were dissolved and corroded. Their mafic minerals are typically replaced by chlorite, hydromica, and iron hydroxides.

The upper Alchan subformation is dominated by andesites in the lower part and rhyolites in the upper part and contains subordinate basaltic andesites and basalts. The andesites contain hornblende and plagioclase phenocrysts embedded in a weakly fluidal glassy groundmass. Hornblende is almost completely replaced by opacite, and plagioclase is saussuritized. The basalts and basaltic andesites typically contain pyroxene and hornblende phenocrysts. In addition to crystal clasts, the andesite tuffs contain numerous clasts of sandstones, dacites, and rhyolites.

The volcanic rocks of the Alchan Formation are typically of normal and moderate alkalinity and show a gradual increase in total alkalis (from 4.5 to 8 wt %) accompanying a SiO_2 increase from basalt to rhyolite. Subalkaline rocks, trachydacites and trachyandesites, occur in subordinate amounts. In the classification diagram SiO_2–FeO*/MgO [20], the basalts, andesites, and dacites of the formation are plotted in the calc-alkaline field with a low FeO*/MgO ratio, whereas the rhyolites and rhyodacites have a high FeO*/MgO ratio and fall within the tholeiite field. The TiO_2 content of the rocks is low and increases from rhyolites (TiO_2 = 0.2–0.4 wt %) to basalts (TiO_2 = 0.9–1.1 wt %). An increase in TiO_2 content is accompanied by a decrease in K_2O content from rhyolites to basalts (Fig. 2). The K_2O/Na_2O ratio varies around 1. All the volcanic rocks of the formation are moderately aluminous and have slightly elevated MgO contents.

The volcanic rocks of the Severyanka Formation are represented by both aphyric and porphyric varieties. With respect to phenocryst assemblages, the basalts and basaltic andesites are divided into the plagioclase–pyroxene and olivine–pyroxene types. Plagioclase is andesine–labradorite and labradorite. Both clinopyroxene and orthopyroxene were detected. The latter is typically replaced by chlorites and iron hydroxides. In addition, the basalts contain olivine phenocrysts and opacitized prismatic plates of hornblende. The groundmass has an intersertal or microdoleritic texture and often an amygdaloidal structure. Based on phenocryst assemblages, the andesites are subdivided into hornblende, pyroxene–hornblende, and pyroxene varieties. The extrusive facies are made up of quartz-bearing hornblende andesites and dacites. The mafic minerals of the andesites are replaced by chlorite, hydromica, and carbonate. The amygdules are filled with chalcedony, carbonate, and chlorite. Some andesites are characterized by the presence of large, partly dissolved quartz xenocrysts rimmed by small grains of clinopyroxene and biotite and high-mg# hornblende. Some andesites contain late hydrothermal veinlets of quartz and noble opal, occasionally concentrating in commercial amounts.

The rocks of the Severyanka Formation show elevated MgO contents (Table 1), with the highest values (6.5–7.5 wt % MgO) being found in the pyroxene–hornblende andesites and basaltic andesites. All rocks show elevated alkalinity and, in contrast to the rocks of the Alchan Formation, a predominance of K over Na (K_2O/Na_2O = 1.3–5.4). In the classification diagrams SiO_2–($Na_2O + K_2O$) (Fig. 2) and SiO_2–FeO*/MgO [20], all the rocks fall into the field of the calc-alkaline

Table 1. Chemical composition of volcanic rocks from the Alchan basin (wt %)

Sample no.	SiO_2	TiO_2	Al_2O_3	Fe_2O_3	FeO	MnO	MgO	CaO	Na_2O	K_2O	P_2O_5	H_2O^-	LOI	Total
Assikaev Formation														
A-406	52.14	0.85	16.58	2.87	4.86	0.12	3.97	6.15	3.00	2.22	0.24	0.29	6.62	99.86
A-407	52.57	0.74	14.50	0.00	3.74	0.12	3.77	7.92	2.86	2.21	0.525	0.28	10.58	99.81
Lower Alchan subformation														
1	71.49	0.23	14.44	4.40	0.40	0.02	0.12	0.61	2.92	3.93	0.10	0.13	1.66	100.45
2	68.43	0.32	14.96	2.48	1.37	0.08	0.51	0.82	3.30	4.85	0.22	0.08	2.26	99.68
3	69.48	0.39	14.46	2.68	0.99	0.05	0.59	0.82	3.22	4.38	0.18	0.09	2.35	99.68
4	68.91	0.23	14.94	2.71	0.73	0.12	0.47	0.77	3.61	4.65	0.53	0.28	2.23	100.18
5	67.92	0.49	14.48	2.72	2.80	0.08	0.27	2.01	4.45	2.74	0.20	0.16	1.25	99.57
6	66.11	0.58	15.57	3.90	1.85	0.05	0.77	1.71	4.53	1.96	0.18	0.16	2.19	99.56
7	63.76	0.59	1557	1.71	5.39	0.11	0.92	2.16	4.16	2.76	0.20	0.08	2.41	99.82
8	63.99	0.54	15.62	1.98	2.38	0.09	1.49	3.04	2.63	3.55	0.20	0.20	3.81	99.52
Upper Alchan subformation														
9	63.05	0.60	16.27	2.77	2.92	0.11	1.75	3.66	2.81	2.36	0.24	0.22	3.47	100.17
10	60.50	0.81	15.35	1.83	2.98	0.14	1.53	4.86	1.76	2.65	0.28	0.19	6.83	99.71
11	60.82	0.65	16.92	2.85	2.99	0.06	0.86	2.03	3.56	4.79	0.22	0.13	3.65	99.53
12	60.42	0.64	16.81	2.80	2.85	0.11	1.43	4.47	3.20	2.36	0.25	0.16	3.98	99.48
13	58.95	0.69	15.40	2.19	3.52	0.09	1.97	4.82	2.20	2.60	0.27	0.34	6.63	99.70
Al-12	59.70	0.67	16.15	3.11	3.77	0.11	5.00	2.67	3.33	2.79	0.23	0.34	1.66	99.88
Al-13	60.60	0.70	16.13	2.28	4.17	0.11	3.48	2.46	3.75	3.83	0.24	0.39	1.85	99.99
Al-14	57.60	0.67	15.48	2.76	3.64	0.11	3.81	2.97	3.58	3.54	0.24	0.36	4.91	99.68
Al-15	57.40	0.72	16.12	2.62	4.81	0.14	4.47	3.93	2.77	2.51	0.24	0.61	3.60	99.94
Al-19	58.50	0.67	16.15	2.42	4.01	0.13	4.80	2.38	3.66	2.87	0.30	0.42	3.49	99.80
Al-20	53.50	1.11	15.87	3.59	3.49	0.11	5.46	4.40	2.00	3.25	0.60	0.40	6.15	99.93
Al-22	52.70	0.88	17.01	5.87	3.78	0.18	7.78	5.12	1.73	2.19	0.30	0.46	1.71	99.71
14	62.97	0.59	16.83	3.42	1.30	0.08	1.80	2.94	4.70	2.80	0.27	0.28	1.85	99.83
Severyanka Formation														
P-2	64.00	0.65	15.68	1.86	2.42	0.10	3.71	1.86	2.09	3.85	0.39	0.53	1.04	99.90
P-5	63.60	0.89	16.30	1.73	3.13	0.09	3.98	1.39	2.41	3.89	0.45	0.87	0.90	99.72
P-7	60.00	0.94	16.00	2.21	3.87	0.13	5.30	3.30	1.24	3.91	0.47	0.76	1.66	99.97
P-8	55.70	1.04	15.92	3.11	4.24	0.11	7.45	2.92	1.30	3.07	0.50	0.53	3.98	99.97
P-9	54.10	1.06	17.22	2.07	4.92	0.16	7.01	2.62	0.58	3.15	0.54	0.68	5.15	99.86
P-10	53.20	1.60	15.89	2.07	5.92	0.17	6.79	3.45	1.73	3.47	0.60	1.34	3.40	99.66
P-11	53.90	1.11	17.19	1.73	6.15	0.11	7.35	3.37	1.30	3.23	0.50	0.77	3.23	99.97
15	50.21	1.78	15.23	5.70	3.42	0.11	5.52	7.04	2.97	2.22	0.40	1.07	3.93	99.60

Note: Basalts of the Assikaev Formation (collection of A.N. Filippov) were sampled in the right bank of the Bikin River east of the settlement of Verkhnii Pereval; samples (1–13) were taken west of Verkhnii Pereval. Samples from 1 to 8 characterize an ignimbrite section of the lower Alchan subformation from bottom to top: (1) sample O-1980a, (2) sample O-1980/1, (3) sample O-1980/1a, (4) sample O-1980/2, (5) sample O-1980/2a, (6) sample O-1980/5, (7) sample O-1980/6, and (8) sample O-1980/8); andesites of the upper Alchan subformation: (9) sample O-1980/3, (10) sample O-1980/11, (11) sample O-1980/10, (12) sample O-1980/13, (13) sample O-1980/14, (14) extrusive andesite, sample O-1980/15). Samples with names starting with 'Al' were taken near the settlement of Znamenka. Samples of the Severyanka Formation were taken along the Severyanka Creek, right tributary of the Alchan River. (15) Sample O-1970/8.

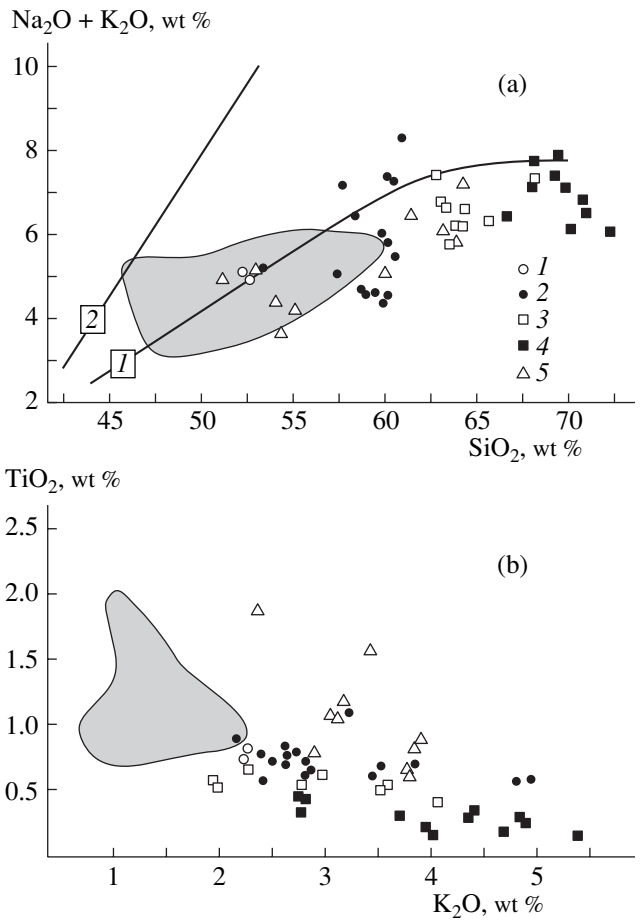

Fig. 2. Compositions of the volcanic rocks of the Alchan basin in the diagrams of (a) $Na_2O + K_2O$)–SiO_2 and (b) TiO_2–K_2O. (*1*) Basalts of the Assikaev Formation (*2–4*) volcanic rocks of the Alchan Formation: (*2*) basaltic andesites and andesites, (*3*) dacites and rhyodacites, and (*4*) rhyolites; (*5*) basalts, basaltic andesites, and andesites of the Severyanka Formation. The lines separating the subalkaline (1) and alkaline (2) series are shown after [19]. Hereafter, the shaded field corresponds to the volcanic rocks of the Korkino Group, Partizanskii basin, Primorie [10].

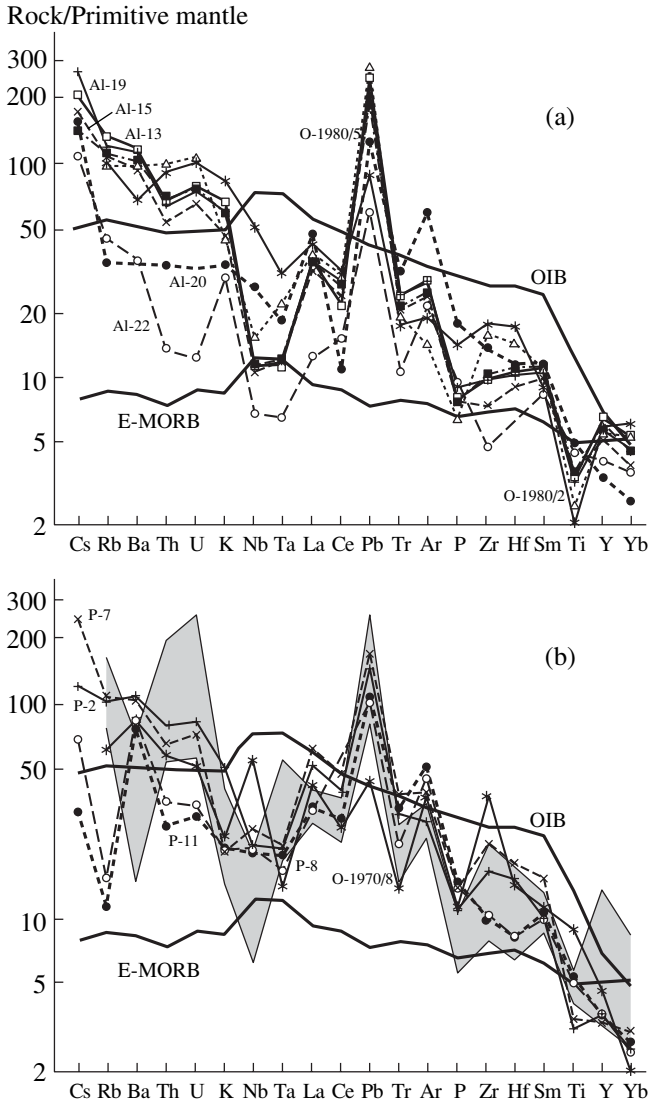

Fig. 3. Incompatible elements in the volcanic rocks of the (a) Alchan and (b) Severyanka formations. The concentrations were normalized to primitive mantle values [35].

series. With increasing SiO_2, FeO*/MgO shows only slight variations from 0.9 to 1.5. In the TiO_2–K_2O diagram, the rocks of the Severyanka Formation are subdivided into two groups. One group includes andesites and andesidacites with K_2O = 3.5–4.0 wt % and TiO_2 < 1 wt %, and the other group includes basaltic andesites and basalts with K_2O = 3.0–3.5 wt % and TiO_2 = 1.0–1.6 wt %. Within these groups, an increase in K_2O content is accompanied by an increase in TiO_2 (Fig. 2). The volcanic rocks of the Severyanka Formation have high P_2O_5 contents (0.39–0.6 wt %), which are significantly higher than those in the andesites and basaltic andesites of the Upper Cretaceous Eastern Sikhote Alin volcanic belt [21]. With respect to the high MgO contents in the rock and hornblende and high contents of K_2O and Cr, the andesites of the Alchan basin are similar to adakites [22].

TRACE ELEMENTS

The basalts of the Assikaev Formation have low contents of compatible elements (Table 2): Ni = 40–55 ppm, Co = 15–30 ppm, Cr = 15–40 ppm, and V = 120–160 ppm. Their concentrations are well correlated with the MgO content of the basalts. There is no data on LILE, HFSE, and REE in these rocks, but the relationships of major elements (for example, TiO_2–FeO and TiO_2–K_2O) and some trace elements (Cr–Ni and Ti–V) are similar to those of island-arc rocks.

The rocks of the Alchan and Severyanka formations have similar trace-element distribution patterns (Table 2, Fig. 3). The concentrations of compatible transition elements (Ni, Co, Cr, and V) are elevated and strongly variable. Chromium content is especially high: up to 130 ppm in the andesites and basaltic andesites of the

Table 2. Trace element composition (ppm) of typical volcanic rocks from the Alchan basin

Element	1	2	3	4	5	6	7	8	9	10	11	12	13	14	15	16
	Formation															
	Assikaev		Lower Alchan			Upper Alchan						Severyanka				
	sample No.															
	A-407	A-408	1	4	5	Al-12	Al-13	Al-15	Al-19	Al-20	Al-22	P-2	P-7	P-8	P-11	15
Cr	15	30	25.10	30.1	27.7	47.1	49.8	106	49.1	127.1	74.3	53.1	125	133	170	110
Ni	43	50	10.50	14.2	16.7	13.1	11.7	19.3	11.6	66.2	26	19.2	67.7	65.7	65	56
Co	25	19	7.9	12.41	8.37	18.14	15.45	11.6	18.4	18.2	23.7	12.3	21.6	22.1	16	25.3
V	154	148	–	–	–	190	180	200	170	130	280	140	150	200	210	180
Rb	5	5	70.5	63.8	58.9	78.9	89.9	70.2	19.1	26.2	63.5	63.5	69.4	9.5	7.5	44.0
Sr	–	–	291	411	310	511	561	460	1201	436	584	584	792	972	1021	854
Ba	–	–	607	519	643	654	806	602	625	225	718	718	732	586	514	560
Hf	–	–	5.17	5.4	4.31	3.19	3.11	2.56	2.99	3.47	1.72	4.75	5.22	2.37	0.42	4.1
Zr	–	–	140	201	184	111	102	76.1	162	51	191	191	239	110	105	192
Y	–	–	25.3	31.1	27.13	27.32	25.97	22.1	14.5	17.1	15.9	15.9	19.5	16	15.8	19
Ta	–	–	0.93	1.21	0.81	0.49	0.66	0.52	0.53	0.71	0.23	0.23	0.82	0.78	0.66	1.2
Nb	–	–	12.4	12.3	10.25	8.35	8.96	7.34	9.96	4.55	14.1	14.3	17.8	14.1	14	14.0
Pb	–	–	19.3	14.5	9.8	15.7	17.8	14.5	18.2	11.6	4.7	13	14.3	8.4	9.4	9.0
Th	–	–	5.81	8.15	7.98	5.30	5.31	4.04	5.30	2.65	1.18	6.42	5.26	2.93	2.33	5.1
U	–	–	2.30	2.18	2.23	1.65	1.65	1.34	1.57	0.68	0.29	1.84	1.51	0.77	0.64	1.1
La	–	–	27.7	28.3	24.5	21.17	22.57	20.29	3.89	9.17	35.3	35.3	40	23.3	25.4	30.0
Ce	–	–	55.3	52.6	50.6	44.32	45.97	40.63	20.9	28.1	67.8	67.8	82.3	51	52	63
Pr	–	–	4.90	5.01	5.35	5.54	5.99	5.22	8.09	2.76	7.75	7.75	9.98	5.83	5.98	8
Nd	–	–	23.4	19.3	22.8	21.85	22.88	21.41	30.2	11.9	28.3	28.3	36.6	23.9	24.3	29
Sm	–	–	4.01	3.97	4.83	5.17	4.63	4.08	5.44	3.42	4.48	4.48	6.73	4.09	5.04	5.1
Eu	–	–	1.20	1.36	1.16	1.20	1.32	1.20	1.52	0.83	1.29	1.29	1.67	1.18	1.28	1.2
Gd	–	–	4.90	5.71	4.68	4.34	4.55	4.20	3.82	3.04	3.75	3.75	4.80	3.85	3.78	4.0
Tb	–	–	0.80	0.75	0.72	0.64	0.64	0.56	0.52	0.48	0.44	0.44	0.58	0.54	0.60	1.0
Dy	–	–	4.83	5.02	4.15	3.73	3.73	3.73	2.88	3.02	2.50	2.50	3.03	2.85	2.92	3.0
Ho	–	–	0.71	0.82	0.77	0.68	0.70	0.61	0.40	0.54	0.39	0.39	0.53	0.48	0.52	1.0
Er	–	–	2.81	3.05	2.47	2.39	2.10	1.76	0.80	1.66	1.20	1.20	1.59	1.43	1.44	2.0
Tm	–	–	0.47	0.51	0.44	0.62	0.57	0.63	0.20	0.30	0.29	0.29	0.40	0.20	0.30	–
Yb	–	–	2.70	2.93	2.71	1.97	2.26	1.68	0.88	1.57	1.08	1.08	1.34	1.07	1.16	1.03
Lu	–	–	0.37	0.39	0.42	0.26	0.33	0.24	0.27	0.10	0.22	0.16	0.25	0.18	0.19	0.12

Note: Sample numbers correspond to those in Table 1.

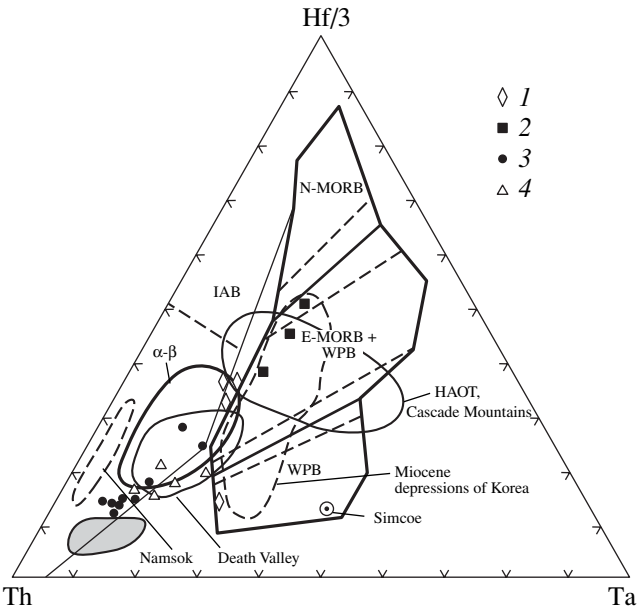

Fig. 4. Th–Hf–Ta diagram for the volcanic rocks of transform margins. Data points: (*1*) Onsupkhen basaltic fields in northwestern Korea, (*2*) tholeiites of the Paektusan, Korea [7], (*3*) volcanic rocks of the Alchan Formation, and (*4*) volcanic rocks of the Severyanka Formation. Compositional fields of various geodynamic settings are after [24]: N-MORB, depleted midocean ridge basalts; E-MORB + WPB, enriched tholeiites of midocean ridges and within-plate tholeiites; WPB, alkali basalts of within-plate structures; and IAB, basalts of island arcs and active continental margins. The compositional fields of rocks from the Cenozoic transform margin of northwestern America (HAOT, high-Al olivine tholeiites), calc-alkaline basalts, basaltic andesites (α–β), and alkali basalts of Simcoe, Cascade Mountains are after [32]. The basalts of the Death Valley, Basin and Range Province are after [30]. The volcanic rocks of the Cenozoic basins of Korea synchronous with strike-slip faulting are after [7].

Alchan Formation and 170 ppm in the rocks of the Severyanka Formation. The variations of these and some incompatible elements (Ti, Zr, Hf, Nb, Ta, Th, U, and REE) are correlated with the MgO content of the rocks. The distribution patterns of LILE are more fractionated than those of HFSE. In terms of Cs, Rb, Ba, Th, U, and K concentrations, the andesites and dacites of the Alchan and Severyanka formations are enriched relative to OIB, whereas the basalts and basaltic andesites are close to E-MORB (Fig. 3). The rocks display distinct negative Ta and Nb anomalies and a positive Sr anomaly typical of island-arc rocks. There is a pronounced positive Pb anomaly, which is characteristic of continental rift basalts. The concentrations of some HFSE (Zr, Hf, and Y) are somewhat higher than those of E-MORB and island-arc basalts, approaching those of within-plate volcanic rocks, and the Ti content is lower than that of E-MORB. The Zr/Nb ratio (7.5–13) is close to that of within-plate basalts (4–12). The ratios of La/Nb (1.7–4), Ba/Nb (37–90), Ba/Th (80–220), Rb/Nb (0.53–10), Th/Rb (16–0.77), Ba/La (18–35), etc. in the volcanic rocks of the Alchan and Severyanka formations are significantly higher than those of the primitive mantle, N-MORB, and OIB of different origin [23] and are comparable with those of the continental crust.

In the Th–Hf–Ta diagram (Fig. 4), the volcanic rocks of the Alchan Formation plot in the island-arc field, whereas the points of the Severyanka Formation are shifted from the island-arc field toward within-plate basalts. The rocks have low Nb/La and Ba/La ratios, which is typical of orogenic andesites. At the same time, in the $(La/Sm)_n$–La/Hf diagram, they occur in the field of within-plate basalts. Their Th/Yb (1.7–5.5) and Ta/Yb (0.2–0.8) ratios are higher than those of oceanic island arc and within-plate ocean island rocks [25] and similar to those of continental margin volcanic rocks (Fig. 5).

The volcanic rocks of the Alchan and Severyanka formations have strongly fractionated REE distribution patterns (La_n/Sm_n = 1.6–4.8, La_n/Yb_n = 3.9–25; Fig. 6). The distribution patterns of the Alchan volcanic rocks fall within the field of the Korkino Group of the Partizanskii basin. However, the Alchan rocks show significant variations in REE contents. In particular, basaltic sample Al-22 from the Alchan Formation (Fig. 6a) has the lowest LREE content and a weak negative Eu anomaly (Eu/Eu* = 0.93), which is presumably caused by plagioclase flotation. In contrast, the distribution pattern of basaltic andesite sample Al-20 is characterized by the highest LREE (La_n/Sm_n = 3.6) and the lowest HREE concentrations (La_n/Yb_n = 24.6) and shows no Eu anomaly. It intersects the distribution patterns of most samples from the Alchan Formation and Korkino Group. The more silicic rocks of the Severyanka Formation are enriched in LREE compared with the basalts and basaltic andesites at similar HREE abundances (Fig. 6b). The volcanic rocks of the Alchan basin show strongly fractionated LREE and MREE patterns (from La to Ho), whereas their HREE patterns are flattened and occasionally even rise from Ho to Lu.

Thus, the rocks of the Alchan and Severyanka formations of the Alchan basin display island-arc, E-MORB, and within-plate geochemical signatures.

GEODYNAMIC INTERPRETATION

The volcanic rocks from the Alchan basin were compared using various discriminant diagrams with the rocks of the Cenozoic transform margin of western North America, strike-slip extensional Cenozoic basins of the Asian continental margin, and Albian–Cenomanian rocks of the Korkino Group, Primorie [10]. Some of these diagrams are shown in Figs. 4 and 5.

The Cenozoic and Recent margins of western North America are structurally similar to the Early Cretaceous and Cenozoic East Asian margin [25]. The western margin of North America in the Mesozoic and Cen-

ozoic was a classic transform margin, which developed owing to the interaction between the Pacific plate and the weakly mobile North American continent [26]. Along the boundary between these two plates, there are the ridge–arc type Californian and Queen Charlotte dextral transform faults, more than 1500 km long each [27]. Laterally, transform slip zones are alternated with subduction segments, which were detected in the Cascade Mountains, where the Juan de Fuca plate plunges beneath the continent and an accretionary prism is formed [28].

Numerous pull-apart basins along the entire fault system and parallel grabens in the Basin and Range Province, including the classic rhomb-shaped graben (pull-apart basin) of Death Valley subsided 85 m below sea level, were formed owing to movements along the Californian strike-slip faults. Dikes, sills, and flows of basalts, andesites, dacites, and rhyolites are confined to the strike-slip extensional basins of the Californian margin. The geochemistry of these volcanic rocks indicates their mixed source, involving deep-seated and crustal melts. The composition of the volcanic rocks strongly depends on the intensity and depth of strike-slip extension in particular basins [29].

The volcanic rocks of the Cascade Mountains are represented by three main end-members: (1) high-Al olivine tholeiites (HAOT) similar to N-MORB; (2) island-arc basalts and basaltic andesites with high LILE and low HFSE and HREE concentrations; and (3) alkali basalts of the Simcoe volcanic center east of Mount Adams, which show within-plate geochemical characteristics [31, 32]. In addition to these rocks, most volcanic centers in the Cascade Mountains contain abundant rocks with mixed geochemical characteristics, which were produced from two or more main magma types. A characteristic feature of these rocks is a sigmoidal REE distribution pattern, which is interpreted as reflecting subduction-related enrichment of the magma source [32].

Studies in the Circum-Japan region showed that Cenozoic magmatic complexes are not related to subduction, as was previously believed, but formed in rift depressions under extensional conditions during activation of dextral displacements along the submeridional and northeastern Sakhalin–Japan fault system. These complexes bear mixed subduction and within-plate signatures [1, 33]. A similar conclusion was drawn by P.I. Fedorov and N.I. Filatova, who studied Cenozoic volcanism in the extension zones of Korea [7–9, 34]. They distinguished four volcanic complexes: (1) Eocene–Oligocene complex exemplified by the shoshonites of the Namsok field, Kilchu–Myongchon graben in northeastern Korea; (2) Miocene rocks of the Onsupkhen field in the northwestern part of Korea and the Pohang–Yangnam graben in southwestern Korea; (3) Pliocene–Quaternary complex with the largest fields (Paektusan, Chilbosang, and Mengang) located in northeastern Korea; and (4) Quaternary complex including separate small fields of alkali basalts filling

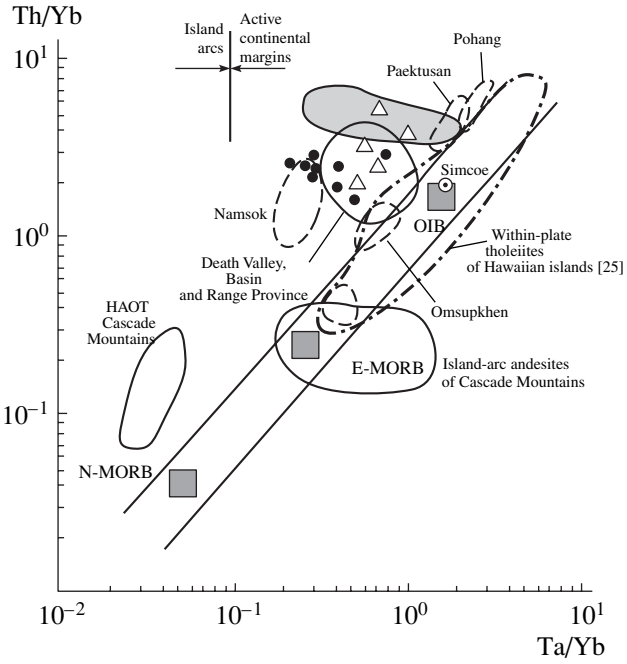

Fig. 5. Diagram Th/Yb–Ta/Yb for the volcanic rocks of transform geodynamic settings. Symbols are the same as in Fig. 4.

grabens in central Korea. During the Eocene–Oligocene stage of the evolution of the Korean region, calc-alkaline basaltoids and within-plate alkaline volcanic rocks were accumulated in inland pull-apart basins. During the Miocene stage, alkali basalts with within-plate and island-arc geochemical signatures (low TiO_2 and relative Ta–Nb depletion) erupted in a slightly extensional environment in the rear parts of the continental margin. The Miocene volcanic rocks that were formed in the near-ocean zones of southeastern Korea affected by the maximum extension become significantly depleted and acquire enriched tholeiite (E-MORB) signatures. The Pliocene–Quaternary and Quaternary magmatism is represented by the bimodal associations of alkaline, moderately alkaline, and tholeiitic series, which are geochemically similar to within-plate complexes but often exhibit island-arc and MORB signatures. Thus, the role of a within-plate source increases with decreasing age and strongly varies in coeval volcanic rocks.

A comparison with the basalts occurring in the continental margin rifts around the Sea of Japan shows that the basalts of the Assikaev Formation of the Alchan basin are most similar to the Oligocene shoshonites of the Namsok Complex of the Kilchu–Myongchon graben in Korea.

In the Th–Hf–Ta diagram (Fig. 4), the samples of the Alchan Formation plot at higher relative concentrations of Hf and Ta compared with the rocks of the Korkino Group. The volcanic rocks of the Severyanka

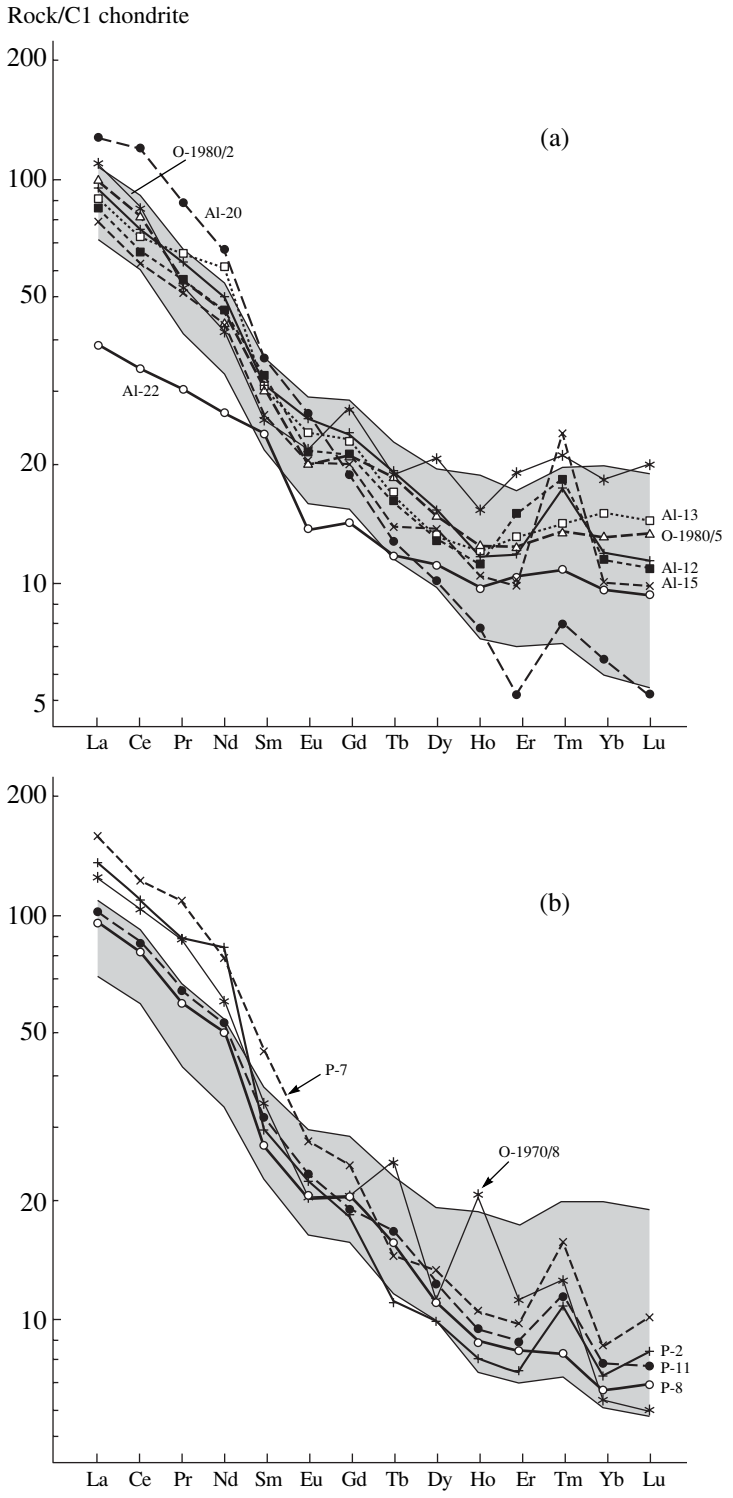

Fig. 6. REE distribution pattern in the rocks of the (a) Alchan and (b) Severyanka formations of the Alchan basin.

Formation are even richer in these elements and shifted toward the within-plate basalt field, into the fields of the Death Valley basalts of the Basin and Range Province and basaltic andesites of the Cascade Mountains. Similar relationships are observed in the $(La/Sm)_n$–La/Hf diagram, where the rocks studied are plotted in the field of within-plate basalts from the Basin and Range Province. In the Th/Yb–Ta/Yb diagram (Fig. 5), most samples from the Alchan Formation fall within the field of the Eocene–Oligocene Namsok Complex, and some

samples of the Alchan Formation and all samples of the Severyanka Formation are shifted towards the within-plate source into the field of rocks from the Death Valley, Basin, and Range Province.

In the Y/Nb–Zr/Nb diagram, the rocks of the Alchan Formation are plotted near E-MORB in the lower part of the field of the Korkino Group, and the volcanic rocks of the Severyanka Formation occupy an intermediate position between E-MORB and OIB in the fields of the Miocene and Pliocene–Quaternary rocks of Korea and the rocks of Death Valley. With respect to Ce/Y–Zr/Nb relations, the rocks of the Alchan Formation occur between the OIB, E-MORB, and N-MORB sources in the field of moderately alkaline Paektusan basalts, and the rocks of the Severyanka Formation with higher Ce/Y values (3.5–4.2) are confined to the Death Valley field.

Thus, with respect to the concentrations, degree of differentiation, and ratios of trace elements, the Cretaceous magmatic rocks of the Alchan basin are similar to the Cenozoic volcanic rocks of the Californian transform margin and strike-slip extensional continental grabens of Korea. At the same time, there are some differences in trace-element distribution between the rocks of the Alchan and Severyanka formations. The former resemble the Miocene and Pliocene–Quaternary complexes of Korea, whereas the latter are closer to the rocks of Death Valley. In our opinion, the compositional variations in the rocks of the Alchan and Severyanka formations and their similarity to the volcanic rocks of typical transform zones in the Cenozoic margins of Asia and North America were caused by tectonic factors and could be related to their derivation from different magma sources variably enriched in trace elements and mixing of magmas from these sources.

Local extensional segments in a transform margin environment may experience breakup of the lithosphere and formation of local trans-lithospheric pull-aparts. The upwelling of a mantle diapir through these pull-apart zones causes melting in the overlying lithosphere and continental crust. Depending on the depth of magma generation and extent of mixing with mantle plume melts, the magmas generated in these zones reflect the degree and depth of melting and display a combination of signatures from different mantle sources [7]. The contributions of different sources (island-arc, within-plate, and MORB) can be qualitatively estimated using the Ba/La–$(La/Yb)_n$ diagram (Fig. 7). It can be seen that the end-member volcanic rock types of the Cascade Mountains and diverse magmatic rocks from the continental rift zones of Korea are strongly heterogeneous. In particular, the composition of Simcoe HAOT from the Cascade Mountains is dominated by the MORB and WPB components. The Namsok shoshonites and the Early Miocene tholeiites of the Yangnam zone of Korea with low $(La/Yb)_n$ display mainly depleted MORB and island-arc signatures [7].

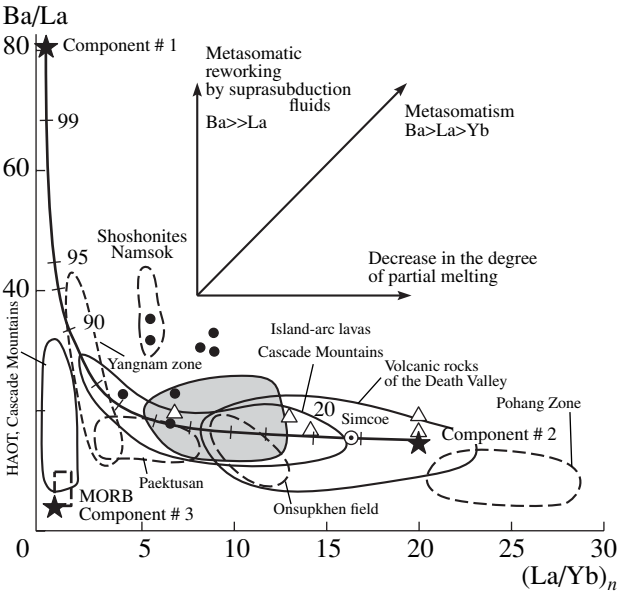

Fig. 7. Diagram Ba/La-$(La/Yb)_n$ for the volcanic rocks of transform geodynamic settings. Component #1: Ba/La = 80 and $(La/Yb)_n$ = 0.5; component #2: Ba/La = 15 and $(La/Yb)_n$ = 20; component #3: depleted compositions, including MORB. Numbers along the mixing curve between components #1 and #2 are the degrees of partial melting. Other symbols are the same as in Fig. 4.

The alkaline rocks of the Pohang area with low Ba/La and $(La/Yb)_m$ values are located in the field of a within-plate source. The island-arc volcanic rocks of the Cascade Mountains and the Death Valley plot along the mixing line between island-arc and within-plate sources. The compositions of volcanic rocks from the Onsupkhen and Paektusan area indicate variable contributions of within-plate and depleted MORB sources.

The volcanic rocks of the Alchan Formation have low $(La/Yb)_n$ ratios and fall mainly above the mixing line between the within-plate and island-arc components in the field of metasomatized compositions, shifting toward the island-arc component. Only one basaltic andesite sample (Al-22) with high $(La/Yb)_n$ and low Ba/La ratios is plotted near the within-plate source. Given the near crustal values of some trace element ratios, the formation of the Alchan magmatic rocks can be attributed to the lower crustal anatexis under the influence of a sublithospheric plume. The contribution of crustal materials to the formation of the volcanic rocks of the Alchan Formation is indicated by the high Sr isotopic ratio of andesites ($^{87}Sr/^{86}Sr = 0.70547$). The ascent of such a plume into the mantle windows in the strike-slip extension zones provided the influx of hot fluids into the upper mantle and crust, causing metasomatic reworking and subsequent generation of initial LILE-enriched silicic magmas followed by increasingly more mafic magmas up to basaltic andesites and basalts with an increasing contribution of the within-plate component. Geologically, this is expressed in the

acid-to-basic succession of volcanics with the appearance of more mafic melts enriched in the within-plate component in the upper parts of the Alchan Formation.

The volcanic rocks of the Severyanka Formation have higher $(La/Yb)_n$ values and are plotted along the mixing line between the island-arc and within-plate components, closer to the latter. Together with their high MgO content and siderophile element enrichment, this suggests that they were formed at deeper levels than the rocks of the Alchan Formation. This is supported by other trace element ratios. In particular, the volcanic rocks of the Alchan Formation show low primitive-mantle-normalized ratios of $(Ce/Yb)_n$ (5–7) and Yb_n (3.2–4.0) [35], which correspond to the 5–10% melting of a mantle material containing 2.5% garnet [36]. The same ratios in the volcanic rocks of the Severyanka Formation $(Ce/Yb)_n = 12–21.6$, $Yb_n = 2.1–2.7$) suggest that they are derivatives of deeper seated peridotites with 4% garnet.

CONCLUSIONS

Volcanic activity in the Alchan pull-apart basin, Primorie, occurred in two stages: middle to late Albian to early Cenomanian and Maastrichtian, corresponding to the periods of maximum displacement along the strike-slip faults of the Tan Lu system in the Asian continental margin. The middle to late Albian to early Cenomanian volcanism is represented by the basalts of the Assikaev Formation and rhyolites, dacites, andesites, basaltic andesites, and basalts of the Alchan Formation. The Maastrichtian magmatism included the intermediate–mafic and mafic lavas of the Severyanka Formation. The characteristic features of the volcanic rocks of both stages are high contents of K and Mg; high HFSE abundances exceeding those of E-MORB; high LILE contents exceeding those of OIB; high $(La/Yb)_n$ ratios; the presence of distinct negative Ta–Nb anomalies and positive Th, U, Pb, and Sr anomalies typical of island-arc magmas. Some trace-element ratios are close to those of the continental crust. The rocks have strongly fractionated LREE and MREE patterns and flattened or even positively sloped HREE patterns. These geochemical characteristics indicate a peculiar composition of the volcanic rocks of the Alchan basin combining the geochemical signatures of depleted, within-plate, and island-arc geodynamic settings, which distinguishes them from the tholeiites and alkaline lavas of continental rifts and oceanic islands and suggests their derivation from several magmatic sources.

The aforementioned indicators suggest that the rocks of the Severyanka Formation are not subduction-related, as was previously believed. The combination of island-arc and within-plate signatures in their composition is indicative of the cessation of Pacific plate subduction beneath the continent and the resumption of strike-slip processes in the continental margin.

A comparison of the Alchan basin rocks with the volcanic rocks of the Californian margin of North America and Cenozoic depressions related to strike-slip extension in Korea allowed us to determine some indicator features of volcanic rocks formed in a transform continental margin setting.

The magmatic rocks of strike-slip extension zones show the signatures of island-arc and within-plate sources; in some cases, when a transform margin adjoins spreading centers, they also display features of depleted MORB sources. In addition to calc-alkaline rocks, these zones contain bimodal volcanic associations. The rocks are characterized by elevated K and Mg contents. The rocks are variably enriched in LILE relative to HFSE, which is typical of island-arc magmas. At the same time, they have high contents of transition compatible elements (Ni, Co, Cr, and V), which are typical of within-plate magmas. The trace-element distribution patterns normalized to MORB or primitive mantle exhibit a negative Ta–Nb anomaly, which is also characteristic of suprasubduction settings. The Ta/Nb ratio of these rocks is lower, whereas Ba/Nb, Ba/La, and La/Yb are higher than those of some MORB and OIB. With respect to trace element relationships, for example, Ta–Th–Hf, Ba/La-$(Ba/La)_n$, $(La/Sm)_n$–La/Hf, and others, they are located in the field of mixing of magmas from different sources (island-arc, within-plate, and depleted). The magmatic rocks of transform settings are often characterized by sigmoid chondrite-normalized REE distribution patterns with LREE enrichment, a minimum at Ho, and slightly enriched or flat distribution of HREE toward Lu.

The appearance of such magmas in the local extension zones of transform margin environments is presumably related to the breakup of a lithospheric plate and formation of local slab windows. Asthenospheric mantle materials ascend through these windows forming a mantle diapir, which causes metasomatism and magma generation in the mantle wedge and lower crust. The melts are formed at the expense of the asthenospheric diapir, oceanic lithosphere, and crustal materials. The mixing of magmas from different sources in variable proportions in the lithospheric chambers provides the appearance of volcanic rocks with mixed geochemical characteristics in transform margins.

ACKNOWLEDGMENTS

This study was financially supported by the Russian Foundation for Basic Research (project no. 02-05-65326)

REFERENCES

1. A. I. Khanchuk, V. V. Golozubov, Yu. A. Martynov, and V. P. Simanenko, “Early Cretaceous and Paleogene Transform Continental Margins (Californian Type) of Russia’s Far East,” in *Tectonics of Asia* (GEOS, Moscow, 1997), pp. 240–243 [in Russian].

2. V. P. Utkin, *Strike-Slip Dislocations, Magmatism, and Ore Formation* (Nauka, Moscow, 1989) [in Russian].
3. V. V. Golozubov, D. W. Lee, and G. L. Amel'chenko, "Role of Horizontal Displacements during Formation of the Razdol'nenskii Cretaceous Epicontinental Basin, Southern Primorie," Tikhookean. Geol. **17**, 14–21 (1998).
4. D. W. Lee, V. V. Golozubov, and B. S. Lee, "Cretaceous Basins of Southeastern Korea Synchronous with Strike-Slip Faulting," Tikhookean. Geol., No. 1, 39–47 (1998).
5. D. W. Lee, "Strike-Slip Fault Tectonics and Basin Formation during the Cretaceous in the Korean Peninsula," Island Arcs **8**, 218–231 (1999).
6. D. Xu, "Basic Characteristics and Tectonic Evolution of the Tancheng–Lujiang Wrench Fault System," in *Tancheng–Lujiang Wrench Fault System*, Ed. by J. Xu (Wiley, New York, 1993), pp. 17–51 (1993).
7. P. I. Fedorov and N. I. Filatova, "Cenozoic Volcanism of Korea," Geokhimiya, No. 1, 3–29 (2002) [Geochem. Int. **40**, 1–25 (2002)].
8. P. I. Fedorov, N. I. Filatova, S. I. Dril, et al., "Cenozoic Volcanism of Southern Korea," Tikhookean. Geol. **21** (2), 94–106 (2002).
9. N. I. Filatova, "Magmatic Evolution of the Japan Basin in Comparison with the Dynamics of Magmatism of Other Marginal Seas," Petrologiya **11**, 255–288 (2003) [Petrology **11**, 230–260 (2003)].
10. V. P. Simanenko, A. I. Khanchuk, and V. V. Golozubov, "First Data on the Geochemistry of Albian–Cenomanian Volcanism in Southern Primorye, Russia's Far East," Geokhimiya, No. 1, 95–99 (2002) [Geochem. Int. **40**, 86–90 (2002)].
11. V. V. Golozubov, G. L. Amel'chenko, D. W. Lee, et al., "Alchan Epicontinental Basin of Cretaceous Age (Northwestern Primorie)," Geotektonika, No. 3, 53–65 (2002) [Geotectonics **36**, 215–226 (2002)]
12. V. V. Golozubov, Extended Abstract of Doctoral Dissertation in Geology and Mineralogy (Moscow, 2004).
13. G. L. Amel'chenko, V. V. Golozubov, E. B. Volynets, and V. S. Markevich, "Stratigraphy of the Cretaceous Alchan Epicontinental Basin, Western Sikhote Alin," Tikhookean. Geol. **20**, 57–71 (2001).
14. D. Engebretson, A. Cox, and R. G. Gordon, "Relative Motions between Oceanic and Continental Plates in the Northern Pacific Basin," Spec. Pap. Geol. Soc. Am **206**, 1–59 (1985).
15. *Geology of the USSR. Primorie* (Nauka, Moscow, 1969), Vol. 32 [in Russian].
16. E. B. Volynets, "Albian Flora of the Alchan Formation, Primorie," in *Proceedings of Scientific Conference on the Occasion of 110th Anniversary of A. N. Krishtofovich, Vladivostok, Russia, 1997* (Dal'nauka, Vladivostok, 1997), pp. 23–24 [in Russian].
17. V. S. Markevich, *Cretaceous Palinoflora of the Northern Part of the Eastern Asia. IGCP Project No. 350* (Dal'nauka, Vladivostok, 1995) [in Russian].
18. P. V. Markevich, V. P. Konovalov, A. N. Filippov, and A. I. Malinovskii, *Lower Cretaceous Deposits of the Sikhote Alin* (Dal'nauka, Vladivostok, 2000) [in Russian].
19. *Classification and Nomenclature of Igneous Rocks* (Nedra, Moscow, 1981), [in Russian].
20. A. Miyashiro, K. Aki, and A. Sengor, *Orogeny* (Wiley, Chichester, 1982; Mir, Moscow, 1985).
21. V. P. Simanenko and A. I. Khanchuk, "Cenomanian Volcanism of the Eastern Sikhote-Alin Volcanic Belt: Geochemical Features," Geokhimiya, No. 8, 866–878 (2003) [Geochem. Int. **41**, 787–798 (2003)].
22. V. G. Sakhno, *Late Mesozoic–Cenozoic Continental Volcanism of East Asia* (Dal'nauka, Vladivostok, 2001) [in Russian].
23. B. L. Weaver, "Trace Element Evidence for the Origin of Ocean-Island Basalts," Geology **19**, 123–126 (1991).
24. D. A. Wood, "The Application of a Th–Hf–Ta Diagram to Problems of Tectonomagmatic Classification and Establishing the Nature of Crustal Contamination of Basaltic Lavas of the British Tertiary Volcanic Province," Earth Planet. Sci. Lett. **50**, 11–30 (1980).
25. F. A. Frey, M. O. Garcia, W. S. Wise, et al., "The Evolution of Mauna Kea Volcano, Hawaii: Petrogenesis of Tholeiitic and Alkaline Basalts," J. Geophys. Res. **96**, 14347–14375 (1991).
26. B. A. Ivanov, *Central Sikhote Alin Fault* (Dal'nevost. Kn. Izd-vo, Vladivostok, 1972) [in Russian].
27. C. R. Scotese, W. J. Nokleberg, J. W. H. Monger, et al., "Dynamic Computer Model for the Metallogenesis and Tectonics of the Circum-North Pacific," Open-File Rept., 01–262 (2001).
28. J. T. Wilson, "A New Class of Faults and Their Bearing on Continental Drift," Nature **207**, 343–347 (1965).
29. M. T. Brandon, M. K. Roden-Tice, and J. I. Garver, "Late Cenozoic Exhumation of the Cascadia Accretionary Wedge in Olympic Mountains, Northwest Washington State," Geol. Soc. Am. Bull. **110**, 985–1009 (1998).
30. Y. Asmerom, S. B. Jacobsen, and B. P. Wernicke, "Variation in Magma Source Regions during Large-Scale Continental Extension, Death Valley Region, Western United States," Earth Planet. Sci. Lett. **125**, 235–254 (1994).
31. T. P. Wagner, J. M. Donnelly-Nolan, and T. L. Grove, "Evidence of Hydrous Differentiation and Crystal Accumulation in the Low-MgO, High-Al_2O_3 Lake Basalt from Medicine Lake Volcano, California," Contrib. Mineral. Petrol. **121**, 201–216 (1995).
32. C. R. Bacon, P. E. Bruggman, R. L. Christiansen, et al., "Primitive Magmas at Five Cascade Volcanic Fields: Melts from Hot Heterogeneous Sub-Arc Mantle," Can. Mineral. **35**, 397–423 (1997).
33. Yu. A. Martynov, *Geochemistry of Basalts of Active Continental Margins and Mature Island Arcs as Exemplified by the Northwestern Pacific* (Dal'nauka, Vladivostok, 1999) [in Russian].
34. N. I. Filatova and P. I. Fedorov, "Cenozoic Magmatism in the Korean–Japanese Region and Its Geodynamic Setting," Geotektonika, No. 1, 54–77 (2003) [Geotectonics **37**, 49–70 (2003)].
35. S. S. Sun and W. F. McDonough, "Chemical and Isotopic Systematic of Oceanic Basalts," in *Magmatism in Ocean Basin*, Ed. by A. D. Saunderas and M. J. Norry, Geol. Soc. Spec. Publ. **42**, 313–345 (1998).
36. T. K. Brandshaw, C. J. Hawkesworth, and K. Gallagher, "Basaltic Volcanism in the Southern Basin Range: No Role for a Mantle Plume," Earth Planet. Sci. Lett. **116**, 45–62 (1993).